THE SCIENTIFIC TEMPER (2026) Vol. 17 (6): 6440-6452

E-ISSN: 2231-6396, ISSN: 0976-8653

Doi: 10.58414/SCIENTIFICTEMPER.2026.17.6.13

https://scientifictemper.com/

RESEARCH ARTICLE

Sparse Optimized Bayesian Learning Algorithm (SOBLA) Based Image Processing Methods in Alzheimer's Disease for Cognitive Impairment

Dr. M. Durairaj[1*], Rajasekhara Babu L[2]

Abstract

Alzheimer's disease (AD) is a chronic mental illness that gradually limits recall, cognitive capacity and daily pursuit. This is why an prompt detection is vital for good clinical management. The traditional diagnostic methods hinge mainly on cognitive evaluations, which often fail to detect the disease in its early stages. Afterwards, MRI has become an important tool for detecting structural brain abnormalities associated with AD and Cognitive Impairment (CI). However, the presence of noise, intensity variations, and motion artifacts in MRI scans can reduce the accuracy of automated diagnostic systems. To overcome these challenges, this study presents an improved MRI-based framework for the detection of AD and CI. The proposed method employs Mean Contrast Limited Adaptive Histogram Equalization (CLAHE) for enhancing image quality and Adaptive Median Filter (AMF) for filtering the noise and reduces the distortions. Then, the Wavelet Transform (WT) is applied to extract significant image features for analysis. To classify, a Sparse Optimized Bayesian Learning Algorithm (SOBLA) combined with Genetic Algorithm (GA)-based parameter optimization is proposed to improve predictive performance. Experimental results on ADNI dataset show that the proposed approach can achieve higher diagnostic accuracy and reliability than existing methods, and thus is suitable for computer aided diagnosis of Alzheimer 's disease.

Keywords: Sparse Optimized Bayesian Learning Algorithm (SOBLA) ,Alzheimer's Disease (AD), Neuroimaging Analysis, Cognitive Decline Detection, Adaptive Median Filtering, Medical Image Enhancement ,Mean Contrast Limited Adaptive Histogram Equalization (MCLAHE) MRI Classification ,Image Preprocessing, Cognitive Impairment Assessment.

Introduction

Alzheimer's disease (AD) is a long lasting and progressive neurodegenerative disorder characterized by the loss of memory, cognition, and reasoning and personality functions. 2 It is one of the main causes of dementia in the elderly worldwide. The ever increasing aging population has made it a great challenge in health-care [A. Dale, 1999], [A. K. Jain, 2002]. AD pathology eventually results in neuronal degeneration and irreversible cognitive impairment that affects an individual's daily functioning and quality of life. Hence, precise early diagnosis and continuous monitoring of disease progression remain important goals in neurological research and clinical practice.

Mild cognitive impairment (MCI) is considered a transition state between normal aging and Alzheimer's disease in general [Barnes DE, 2011]. Not all individuals diagnosed with MCI necessarily progress to dementia, but patients who are cognitively impaired are at a significantly greater risk for developing AD. MCI's heterogeneous nature [Barnes, L.L, 2006] makes it difficult to identify reliable biomarkers to predict disease progression. Thus, considerable efforts are undertaken to develop diagnostic systems based on neuroimaging and computational methods, which can identify subtle cognitive abnormalities

[1]Associate Professor in School of Computer Science, Engineering and Applications, Bharathidasan University, Tiruchirappalli-620023, Tamil Nadu, India

[2]Research Scholar, School of Computer Science, Engineering and Applications, Bharathidasan University, Tiruchirappalli-620023, Tamil Nadu, India

***Corresponding Author:** Dr. M. Durairaj, Associate Professor in School of Computer Science, Engineering and Applications, Bharathidasan University, Tiruchirappalli-620023, Tamil Nadu, India, E-Mail: rajasekharanmca@gmail.com

How to cite this article: Durairaj, M., Babu, R.L. (2026). Sparse Optimized Bayesian Learning Algorithm (SOBLA) Based Image Processing Methods in Alzheimer's Disease for Cognitive Impairment. The Scientific Temper, **17**(6):6440-6452.

Doi: 10.58414/SCIENTIFICTEMPER.2026.17.6.13

Source of support: Nil

Conflict of interest: None.

© *The Scientific Temper. 2026*

Received: 11/06/2026 **Accepted:** 22/06/2026 **Published:** 25/06/2026

at the earliest stages of the disease. Some studies have also demonstrated the importance of preventive strategies and early intervention to reduce the long-term prevalence of dementia and Alzheimer's disease [Bondi, M.W., 2005].

Traditional diagnostic approaches primarily depend on neuropsychological evaluations and cognitive assessment procedures. However, these clinical methods may not always provide reliable outcomes during the initial stages of Alzheimer's disease because cognitive symptoms often emerge gradually and vary significantly among individuals [Cha Sung-Hyuk, 2009]. Subjective memory complaints are frequently considered preliminary indicators of cognitive decline; however, their interpretation may be influenced by demographic, emotional, educational, and psychological factors [D. Wipf, 2011]-[D. Zhang and D. Shen, 2012].

Advances in medical imaging technologies have greatly facilitated the analysis of neurodegenerative disorders. Of these techniques, one of the most effective modalities to examine structural abnormality associated with Alzheimer's disease is Magnetic Resonance Imaging (MRI). The MRI analysis enables visualization of neuroanatomical changes associated with cognitive impairment such as cortical atrophy, tissue degeneration, and ventricular enlargement. In recent years, much attention has been paid to machine learning and automated classification approaches to assist clinicians to diagnose Alzheimer's disease using MRI [Ekstrom, Michael P, 2012]. Compared with traditional manual assessment methods, computer-aided diagnostic systems can improve diagnostic consistency, reduce subjective interpretation errors, and improve clinical decision-making [H. Zou and T. Hastie, 2000].

The Alzheimer's disease Neuroimaging Initiative (ADNI) has greatly contributed to accelerate neuroimaging research by providing standardized MRI datasets and corresponding medical knowledge for the analysis of Alzheimer's disease [Holtzman DM, Morris JC, 2011]. Based on these datasets, several predictive frameworks have been built by researchers to estimate cognitive performance and disease progression given neuroimaging biomarkers. In particular, regression-based learning models and sparse machine learning techniques have shown promising performance to predict clinical cognitive scores from MRI-derived features [Jack, C.R., Bernstein, 2008].

Despite substantial advancements in MRI-based predictive analysis, several challenges still limit the effectiveness of existing computer-aided diagnostic systems. MRI scans are frequently affected by noise, low contrast, intensity inhomogeneity, acquisition-related distortions, and motion artifacts, which may negatively influence feature extraction and classification performance. Consequently, robust preprocessing and discriminative feature extraction techniques are necessary to improve image quality before classification. Furthermore, accurately modelling the nonlinear relationships between neuroimaging biomarkers and cognitive decline continues to remain a complex research problem.

Motivated by these limitations, this study proposes an improved MRI-based diagnostic framework for AD prediction and memory loss analysis. The proposed system integrates image enhancement, image denoising, feature extraction, and sparse Bayesian classification techniques to improve the reliability of prediction and the accuracy of diagnosis. The framework aims to achieve improved performance in computer-aided diagnosis of Alzheimer's disease and cognitive impairment by combining optimized preprocessing methods with a Sparse Optimized Bayesian Learning Algorithm (SOBLA).

Literature Review

Automated Alzheimer's disease (AD) analysis has been greatly enhanced by recent advances in neuroimaging and machine learning techniques. Many studies have focused on the identification of reliable biomarkers from Magnetic Resonance Imaging (MRI) data for the prediction of cognitive decline and disease progression. Various computational approaches have been investigated in the literature to improve the diagnostic accuracy and predictive reliability, including regression models, sparse learning methods, Bayesian inference methods, and multimodal data integration frameworks [Jack, C.R., Bernstein, 2008]–[Petersen, R.C, 2009].

We studied the association between structural MRI features and neuropsychological assessment scores in patients with Alzheimer's disease [Jack, C.R, 2008] by Christopher M. Stonington and colleagues. Their approach used Relevance Vector Regression (RVR) to predict clinical cognitive scores directly from MRI measurements. The experimental results showed a strong correlation between the predicted and observed scores and demonstrated the utility of the machine learning methods for the assessment of cognitive conditions. The study also pointed out the potential of MRI biomarkers to help early diagnosis of dementia.

Yun Wang proposed a high-dimensional regression framework designed to establish mappings between medical imaging features and continuous clinical variables [Khachaturian, Z.S., 2008]. Their method combined adaptive regional feature extraction with nonlinear regression modeling to improve estimation capability for large neuroimaging datasets. Relevance Vector Machines (RVM) were employed to construct predictive mappings capable of handling high-dimensional feature spaces more effectively than traditional Support Vector Regression (SVR) approaches. The reported findings demonstrated improved generalization and predictive performance.

Li Shen proposed a Sparse Bayesian Learning (SBL) method to identify discriminative neuroimaging biomarkers for prediction of Alzheimer's disease [Klöppel, S, 2008].

They used Automatic Relevance Determination (ARD) to extract informative features from MRI and reduce the impact of redundant and less important variables. The Bayesian framework for simultaneous feature selection and classification enhanced the prediction robustness and efficiently captured the structural brain abnormalities linked to the disease.

Jing Wan developed a sparse Bayesian multi-task learning approach for the prediction of cognitive outcomes based on neuroimaging measurements, further improving the predictive modeling [Kloppel, S, 2008]. The framework exploited correlations among multiple cognitive variables and used sparsity constraints to improve feature selection. The model trained on a set of related prediction tasks simultaneously improved prediction accuracy and interpretability of biomarkers related to the progression of Alzheimer's disease.

Zhang and Shen suggested a multi-task learning framework for jointly solving regression and classification problems across heterogeneous biomedical datasets [Korolev IO, 2014]. They used multiple imaging modalities together to improve the consistency of predictions and the sensitivity of diagnosis. Shared feature selection mechanisms were used to find common discriminative features across modalities, thereby improving classification and regression performances.

In another study, Zhang and Shen studied the application of longitudinal and multimodal biomarkers to predict future clinical changes in patients with Mild Cognitive Impairment (MCI) [L. Lin, 2014]. They examined temporal differences in the neuroimaging data collected at different time points. The framework improved prediction of future cognitive deterioration over static predictive models with the longitudinal feature analysis with multimodal learning techniques.

M. R. Sabuncu and K. Van Leemput introduced the Relevance Voxel Machine (RVoxM), a Bayesian-based framework for image-oriented prediction tasks, for neuroimaging applications [N. M. Razali,2011]. Different from the traditional voxel-based methods, RVoxM automatically optimized the parameters of the model in the training process and outputted the probabilistic prediction. The framework showed high predictive power and at the same time detected biologically meaningful voxel-level patterns related to Alzheimer's pathology.

Maria Vounou et al. analyzed sparse Reduced-Rank Regression (sRRR) for identifying associations between genetic factors and voxel-wise longitudinal neuroimaging phenotypes in studies of Alzheimer's disease [P. J. Bickel and E. Levina, 2008]. The authors used penalized multivariate regression to analyze large imaging and genomic datasets together. The proposed framework successfully identified salient associations between genetic markers and structural brain changes, highlighting the potential of sparse multivariate approaches for the analysis of neurodegenerative disease.

Later, Wan et al. [Petersen, R.C., 2009] proposed a correlation-aware and nonlinearity-aware sparse Bayesian learning framework to identify neuroanatomical biomarkers associated with cognitive impairment in Alzheimer's disease. Their work addressed the limitation of traditional linear sparse models by modeling both the structured dependencies among regression coefficients and the nonlinear relationships. For neuroimaging-based cognitive assessment, the framework achieved better predictive accuracy and underscored the need for simultaneous modeling of sparsity, correlation, and nonlinear interactions.

Existing methods have achieved promising results in predicting Alzheimer's disease and assessing cognitive function, but there are still several limitations that need to be addressed. Many techniques are subject to common issues such as MRI noise, intensity inhomogeneity, acquisition artifacts and motion-related distortions, which may adversely impact the reliability of prediction and the performance of classification. Furthermore, accurately modeling nonlinear interactions among neuroimaging biomarkers remains an open research problem. Therefore, there is an urgent need to develop robust preprocessing strategies in combination with optimized sparse Bayesian learning frameworks to improve the reliability and efficiency of computer-aided Alzheimer's disease diagnosis systems.

Proposed Methodology

We propose a new framework for image enhancement and image denoising to improve the quality of input image samples and remove unwanted noise components. The image pre-processing stage generally consists of two steps i.e. image enhancement and image denoising. First, Mean Contrast Limited Adaptive Histogram Equalization (MCLAHE) is applied for enhancing the contrast and visual quality of the MRI images. The image samples are then processed by an Adaptive Median Filter (AMF) to remove noise and minimize the effects of non-uniformity noise, image intensity variations, in-homogeneity and blurring due to image acquisition and patient motion.

The pre-processed denoised Magnetic Resonance Imaging (MRI) images are applied to the Wavelet Transform (WT) to extract the prominent features. We finally develop a sparse multivariate regression framework with a Sparse Optimized Bayesian Learning Algorithm (SOBLA) classifier for accurate prediction and classification. The proposed SOBLA classifier employs a self-tuning mechanism where the Genetic Algorithm (GA) with cross-validation is used to automatically optimize the parameters of the sparse regression algorithm. Experimental analysis based on the Alzheimer's disease Neuroimaging Initiative database shows

that the proposed method outperforms recent competitive techniques in terms of prediction performance.

Mean of Adaptive Histogram Equalization-Contrast Limited (MCLAHE)

Histogram Equalization (HE) is a popular image enhancement method that redistributes the pixel intensity values across the available grayscale range to equalize the contrast distribution of MRI images [Pishvaee, M.S.,2009], [R. C. Gonzalez, 2005]. HE helps to increase the interpretability of neuroimaging features by improving the visibility of anatomical structures in low-contrast regions in MRI analysis of Alzheimer's disease. However, traditional global histogram equalization techniques often lead to over enhancement and intensity distortion in uniform regions of the picture.

To tackle these problems, the local contrast of the image is enhanced by applying Adaptive Histogram Equalization (AHE) separately to small regions of the image. However, standard AHE may improve the noise in relatively homogeneous areas of MRI images. This is why Contrast Limited Adaptive Histogram Equalization (CLAHE) is used to limit over enhancement and retain important structural information [Reisberg, B., 2010]. In CLAHE, the MRI image is divided into several non-overlapping regions called tiles and histogram equalization is applied on each tile independently instead of processing the image globally.

The enhancement operation adjusts the local intensity distribution within each tile according to a predefined histogram mapping function. To avoid excessive amplification of noise components, a clipping threshold is introduced to limit the histogram height. After clipping, the redistributed histogram values are normalized, and neighbouring tiles are combined through bilinear interpolation to minimize artificial boundary discontinuities between adjacent regions.

Let the histogram of an MRI image with grayscale intensity levels in the range [0,L-1] be represented as:

$$h\left(r_k\right) = no_k \tag{1}$$

In the above equation, r_k is the intensity value of k^th gray level of MRI image and no_k is the number of total pixels corresponding to intensity level r_k [25]. The following can be used to equalize the histogram of the image:

$$po_r\left(r_k\right) = \frac{no_k}{MN} k = 0,\ldots L-1 \tag{2}$$

⟦po⟧_r (r_k) is the estimated probability of the occurrence of the intensity level r_k in the MRI image. The sum of all components of normalised histogram is 1. Histogram Equalization (HE) is a commonly used image processing technique for contrast enhancement based on histogram distribution of MRI images. The main objective of this method is to enhance the global contrast by converting the original histogram into an almost uniform distribution, thus obtaining a more balanced distribution of pixel intensities over MRI image. The transformation of histogram equalization can be expressed as:

$$s_k = (L-1)\sum_{j=0}^{k} po_r\left(r_j\right) k = 0,1,\ldots L-1 \tag{3}$$

Here s_k is transformed histogram distribution after equalization of histogram. The CLAHE enhancement procedure is a sequence of operations. First, the MRI image is segmented into several non-overlapped regions of approximately equal size. Then, the histogram of each region is computed independently. A clipping threshold is chosen to limit the over-application of the histogram depending on the level of contrast enhancement required. Once the threshold is set, each local histogram is redistributed so that the histogram height does not exceed the pre-defined clip limit. The value of the clip limit parameter β is calculated as follows:

$$\hat{a} = \frac{MN}{L}\left(1 + \frac{\alpha}{100}\left(s_{max} - 1\right)\right) \tag{4}$$

Here, α is the clip factor determining the degree of contrast enhancement in the CLAHE process. The limit for clip factor zero is MN/L. On the other hand, if the clip factor is set to 100, the maximum possible slope is s max. But choosing just the largest allowable slope does not always provide the best clipping threshold for good image enhancement. The clip limit parameter is also estimated considering the mean intensity value and maximum intensity distribution of the MRI image to make the clipping process better.

The mean value is one of the most popular statistical measures for the determination of the central intensity distribution in CLAHE based enhancement. In MRI image processing, the arithmetic mean is calculated by dividing the total pixel intensity values by the total number of intensity elements in the image.

$$s_{\hat{1}} = \frac{1}{no_k}\sum_{i=1}^{no_K} x_i = \frac{x_1 + x_2 + \ldots . x_{no_k}}{no_k} \tag{5}$$

To further improve the stability and enhancement performance of the CLAHE process, consider a set of intensity values $\{x_1, x_2, x_3 \ldots . x_N\}$ associated with their corresponding frequencies $\{fr_1, fr_2, fr_3 \ldots . fr_N\}$, where the intensity value x_i occurs fr_i times within the MRI image matrix. Based on these intensity-frequency pairs, the mean value $\hat{1}$ can be determined using the following expression:

$$s_{\hat{1}} = \frac{1}{no_k}\sum_{i=1}^{no_K} fr_i x_i = \frac{fr_1 + fr_2 + \ldots . fr_{no_k}}{no_k} \tag{6}$$

The modified clipping limit parameter β_{new} used in the proposed MCLAHE approach is defined as follows:

$$\hat{a}_{new} = \frac{MN}{L}\left(1+\frac{\alpha}{100}\left(\left(\frac{s_i + s_{max}}{2}\right)-1\right)\right) \quad (7)$$

The pixel intensities are transformed by performing linear interpolation between the mappings results obtained from the four neighboring regions. This interpolation process ensures smooth transitions between adjacent image tiles and minimizes artificial boundary effects in the enhanced MRI image [Risacher, S.L, 2009].

$$\mathrm{cdf}_i\left(r_k\right) = \frac{no_k}{N} \quad (8)$$

$$CDF_k\left(r_k\right) = \sum_{j=0}^{k} cdf_i\left(r_j\right) \quad (9)$$

Finally the Cumulative Distribution Function (CDF) for contrast limited histogram is calculated and used for grayscale intensity mapping in enhanced MRI image.

Adaptive Median Filter (AMF)

Adaptive Median Filtering (AMF) is a nonlinear image denoising algorithm that has been widely applied to suppress impulse noise and preserve important anatomical structures in MRI images [S. Zhang, 2005]. In contrast to the traditional linear smoothing filters, the AMF adaptively varies the size of the filtering window according to the local image properties, thus improving the ability of noise removing without producing significant blurring effects. This approach is especially beneficial in MRI pre-processing for decreasing acquisition noise, intensity irregularities, and motion-related distortions while retaining edge information and fine structural details.

The conventional Median Filter (MF) replaces the centre pixel in a local neighbourhood window with the median intensity value of all pixels in the filtering region. The filtering operation is written as

$$f\left(i,j\right) = median\left\{x\left(s,t\right)\right\}$$

where $x(s,t)$ denotes the set of pixel intensity values within the filtering window centered at the spatial location (i,j).

Although the conventional median filter performs effectively under low-noise conditions, its denoising capability decreases when the MRI image contains high-density impulse noise. To overcome this limitation, the Adaptive Median Filter dynamically expands the processing window based on the local noise distribution. This adaptive mechanism enables efficient suppression of corrupted pixels while preserving significant structural and edge-related information.

For each selected filtering window, the following parameters are computed:

Z_{min} : Minimum gray-level intensity value within the neighbourhood window

Z_{max} : Neighbourhood window maximum gray level intensity value

Z_{med} : Gray Level Median Intensity Value of Neighbourhood Window

Z_{xy} : Gray-level intensity of the center pixel

S_{max} : Maximum allowable window size

The AMF algorithm operates in two sequential stages referred to as Level A and Level B.

At Level A, the algorithm determines whether the median value corresponds to a valid image pixel or noise component. The following conditions are evaluated:

$$A_1 = Z_{med} - Z_{min}$$

$$A_2 = Z_{med} - Z_{max}$$

If $A_1 > 0$ and $A_2 < 0$, the median value is considered noise-free and the algorithm proceeds to the second stage. Otherwise, the filtering window size is increased adaptively until either a valid median value is identified or the maximum allowable window size is reached.

At Level B, the algorithm verifies whether the center pixel itself is corrupted by noise. The following expressions are computed:

$$B_1 = Difference\,between\,Z_{xy}\,and\,Z_{min}$$

$$B_2 = Difference\,between\,Z_{xy}\,and\,Z_{max}$$

If B_1 > 0 and B_2 < 0, the original center pixel is kept as it is supposed to be noise-free. Otherwise, the center pixel is replaced by the median value Z_{med}.

With the adaptive window expansion strategy, the AMF can suppress the high-density impulse noise more efficiently than the conventional median filtering methods, while preserving the structural integrity of the image. However, too large windows can decrease the sharpness of the image and remove fine anatomical details [Sabuncu, M.R, 2012]. Thus, selecting a proper maximum window size is important to balance the trade-off between noise reduction and structural preservation in MRI-based Alzheimer's disease analysis.

Wavelet Transform (WT)

Wavelet Transform (WT) is an efficient multiresolution signal analysis technique widely employed in medical image

processing because it simultaneously represents image information in both spatial and frequency domains [Sasi, N.M. and Jayasree, 2013]. In Alzheimer's disease MRI analysis, WT facilitates the extraction of localized texture information, structural irregularities, and frequency-dependent characteristics that are useful for disease prediction and classification. Compared with conventional transform methods, wavelet-based decomposition provides better localization of image features across multiple resolution levels, enabling detailed analysis of subtle neuroanatomical variations.

The WT procedure decomposes MRI images into several frequency subbands containing distinct structural and textural information. The resulting wavelet coefficients preserve localized spatial details together with frequency characteristics, making them highly suitable for biomedical feature extraction tasks. Since adjacent MRI pixels generally exhibit strong spatial correlation, wavelet coefficients effectively represent tissue-specific structural variations associated with neurodegenerative abnormalities.

The wavelet basis functions are generated from the prototype function called the mother wavelet. The multiscale signal representation is obtained by translation and scaling of a family of wavelet functions. The wavelet function can be expressed mathematically as:

$$\mu_{a,b}(t) = \frac{1}{\sqrt{a}}\mu\left(\frac{t-b}{a}\right) \tag{11}$$

Where n an is the scale parameter controlling the dilation of the wavelet function and b is the translation parameter shifting the wavelet along the signal domain.

The proposed framework uses two-dimensional discrete Wavelet Transform on MRI images to produce multi-level decomposition. This operation decomposes the image into four frequency subbands [Low-Low (LL), Low-High (LH), High-Low (HL) and High-High (HH)]. The LL component contains low frequency approximation information about the general anatomical structure of the MRI image while the LH, HL and HH subbands contain horizontal, vertical and diagonal detail information respectively. Multi-level decomposition allows to extract discriminative texture characteristics related to tissue abnormalities in Alzheimer disease.

After decomposition, the generated subband images are combined to construct the final feature representation utilized for classification. For an n-level decomposition process, the cascading feature extraction operation is represented as:

$$F = \{LL_n, LH_n, HL_n, HH_n\} \tag{12}$$

where F represents the extracted feature vector corresponding to the MRI image and n denotes the level of wavelet decomposition.

The extracted wavelet features have large amount of information about intensity distribution, texture variation and spatial characteristics of MRI scans. The features are then passed through the Sparse Optimized Bayesian Learning Algorithm (SOBLA) classifier to improve the prediction and classification efficiency for Alzheimer's disease detection. The proposed framework effectively enhances feature representation and enables more accurate computer-aided diagnosis by using Wavelet Transform in the preprocessing stage.

Sparse Optimized Bayesian Learning Algorithm (SOBLA)

The proposed Sparse Optimized Bayesian Learning Algorithm (SOBLA) is developed based on the theoretical foundation of Sparse Bayesian Learning (SBL) [Shen, L.,

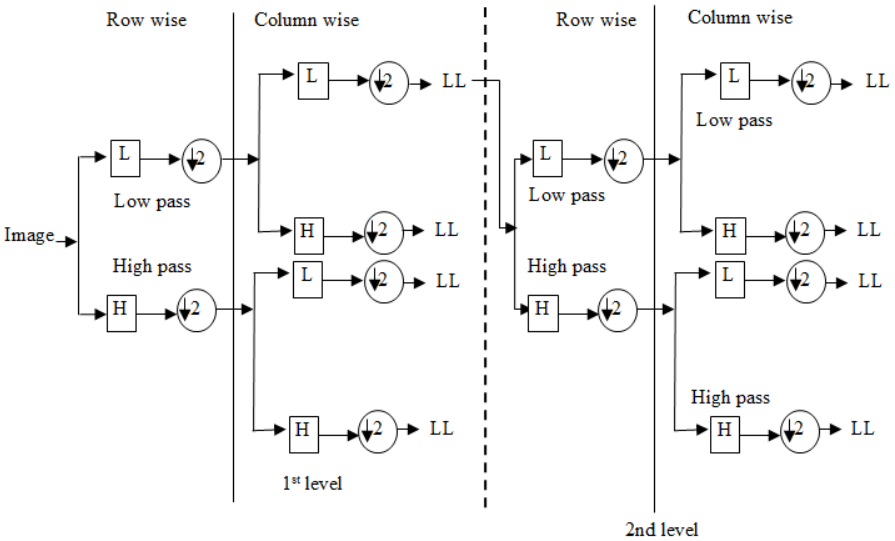


Figure 1: Two-level discrete wavelet transform working principle

2010], a probabilistic sparse modelling framework for variable selection and sparse signal recovery problems. In particular, SBL is useful if only a small subset of variables are relevant for the prediction process. Wipf and Rao previously showed that sparse Bayesian formulations can offer better robustness and sparsity control than many traditional minimization-based approaches, including Lasso-related methods [Shen, L,2010], [Slavin, M.J, 2010].Initially, the regression formulation is transformed into a block sparse representation expressed as:

$$Y=\Phi X+V \tag{13}$$

where Y represents the observed measurement matrix, Φ denotes the sensing matrix, X corresponds to the sparse coefficient matrix, and V represents additive noise components.

The posterior probability distribution of the sparse coefficient matrix is estimated using Bayesian probabilistic modeling techniques. The posterior formulation can be expressed as:

$$\pi\left(X|Y;\Theta\right)=\frac{\pi\left(Y|X;\Theta\right)\pi\left(X;\Theta\right)}{\pi\left(Y;\Theta\right)} \tag{14}$$

Here Θ stands for the whole parameter set associated with the Bayesian setting.

The covariance matrix for the sparse coefficient estimate is given by:

$$\Sigma=\left(\Gamma^{-1}+\frac{\Phi^{\mathrm{T}}\Phi}{\lambda}\right)^{-1} \tag{15}$$

The covariance relationship is further represented as:

$$\Sigma_y=\lambda\mathrm{I}+\Phi\Gamma\Phi^{\mathrm{T}} \tag{16}$$

The corresponding posterior mean estimation is given by:

$$\mu=\ \Gamma\Phi^{\mathrm{T}}\left(\lambda\mathrm{I}+\Phi\Gamma\Phi^{\mathrm{T}}\right)^{-1}Y \tag{17}$$

The sparse coefficient estimation can additionally be represented as:

$$\hat{X}=\mu \tag{18}$$

After the estimation of the model parameters, the MAP estimate is obtained by using the posterior mean distribution of the sparse coefficient matrix:

$$X_{MAP}=\mu \tag{19}$$

To estimate optimal sparse parameters, the proposed framework employs a Type-II maximum likelihood optimization strategy [Shen, L, 2010]. The associated objective function is represented as:

$$L\left(\Theta\right)=log\left|\Sigma y\right|+Y^{T}\Sigma_{y}^{-1} \tag{20}$$

The optimization condition is further represented as:

$$\Theta^{*}=\arg min_{\Theta}L\left(\Theta\right) \tag{21}$$

The learning rules of covariance estimation and sparse coefficient optimization are updated by iteratively minimizing the objective function with respect to the sparse Bayesian parameters:

$$\gamma_i=\frac{1}{d_i}\mathrm{T}r\left[B_i^{-1}(\Sigma_x^i+\mu_x^i\left(\mu_x^i\right)^{\mathrm{T}})\right] \tag{22}$$

$$B_i=\frac{\Sigma_x^i+\mu_x^i\left(\mu_x^i\right)^{\mathrm{T}}}{\gamma_i} \tag{23}$$

$$\lambda=\frac{Y-\Phi\mu_F^2}{N}+\frac{1}{N}\Sigma_i\mathrm{T}r\left(\Sigma_x^i\left(\Phi^i\right)^T\Phi^i\right) \tag{24}$$

$$\Sigma_x=\left(\Gamma^{-1}+\frac{1}{\lambda}\Phi^{\mathrm{T}}\Phi\right)^{-1} \tag{25}$$

$$\mu_x=\Gamma\Phi^{\mathrm{T}}\left(\lambda\mathrm{I}+\Phi\Gamma\Phi^{\mathrm{T}}\right)^{-1}Y \tag{26}$$

The successive column vectors associated with the i^{th} sparse block are represented as:

$$\Phi=\left[\Phi_1,\Phi_2,\ldots.\Phi_g\right] \tag{27}$$

Where Φ_i denotes the group of successive columns corresponding to the i^{th} sparse block in the sensing matrix.

The block diagonal covariance structure corresponding to the sparse Bayesian representation is expressed as:

$$\Gamma=diag\left(\gamma_1B_1,\gamma_2B_2,\ldots,\gamma_gB_g\right) \tag{28}$$

Where B_i represents the covariance matrix associated with the i^{th} block, and γ_i denotes the sparsity-controlling hyperparameter corresponding to that block. The block diagonal covariance representation enables efficient modeling of intra-block correlations within the Sparse Bayesian Learning framework while preserving numerical stability during parameter evaluations.

When the number of measurement vectors is small, estimating the latent covariance matrices becomes more and more difficult. The proposed framework also incorporates covariance regularization and normalization schemes for enhanced estimation stability and numerical robustness Under the low-noise condition, the contributions of the noise covariance can be neglected to some extent, in order to simplify the parameter estimation and reduce the instability during optimization.

The covariance normalization process is represented as:

$$\hat{B}=\frac{B}{B_F}+\epsilon I \tag{29}$$

where ϵ represents a positive regularization parameter introduced to suppress instability caused by noise covariance estimation.

To model short-range correlations among sparse coefficients, the proposed framework utilizes a Toeplitz covariance structure [Stonnington, 2010], [Vounou, M, 2012], expressed as:

$$B = Toeplitz(1, r, r^2, \ldots, r^{n-1}) \quad (30)$$

to fairly accurate A_i, here $\rho_i = \frac{m_1}{m_0}$ with m_0 (resp m_1) is known as the average of entries along the main diagonal (resp. the main sub-diagonal) of A_i. γ_i is known as the standardized approximation of A_i. This Toeplitz structure (30) is a widely used standardized covariance structure [Stonnington, 2010-Vounou, M., 2012]. It has entries that decay exponentially away from the diagonal and therefore models short range correlations. Even with more composite structures they need a lot of parameters and are more difficult to guesstimate. These parameters may lead to errors which may greatly affect the performance of the algorithm. The parameters in Equations (19), (22), (26) and (29) are very important for the performance of the Sparse Bayesian Learning (SBL) algorithm. However, determining the optimal values of these parameters is a highly challenging optimization problem. To address this issue, the proposed method incorporates a Genetic Algorithm (GA) for optimizing parameters such as $IN, \gamma_i, \lambda_i, B^+$. The primary objective of the GA is to identify near-optimal parameter combinations that improve the prediction capability and convergence performance of the SBL framework.

The parameter search space of SBL is very large and complex, and therefore, conventional optimization methods may prematurely converge to local minima before exploring the entire solution space for the global optimum. This limitation is efficiently overcome by the Genetic Algorithm, which performs evolutionary optimization based on the population, by iteratively applying selection, crossover and mutation operations. The proposed SOBLA framework thus provides better parameter tuning and improved classification performance. Algorithm 1 summarizes the overall steps of the SOBLA optimization procedure.

Figure 2. Shows the main operations of the Genetic Algorithm (GA) i.e. population selection and cross over optimization. The selection mechanism is responsible for finding suitable parameter combinations within the Sparse Bayesian Learning (SBL) framework in order to achieve better classification solutions. The proposed method, uses a number of selection mechanisms such as elite selection, roulette wheel selection, rank selection and tournament selection.

In the case of elite selection, the best-performing SBL parameter sets from the Alzheimer's disease sample

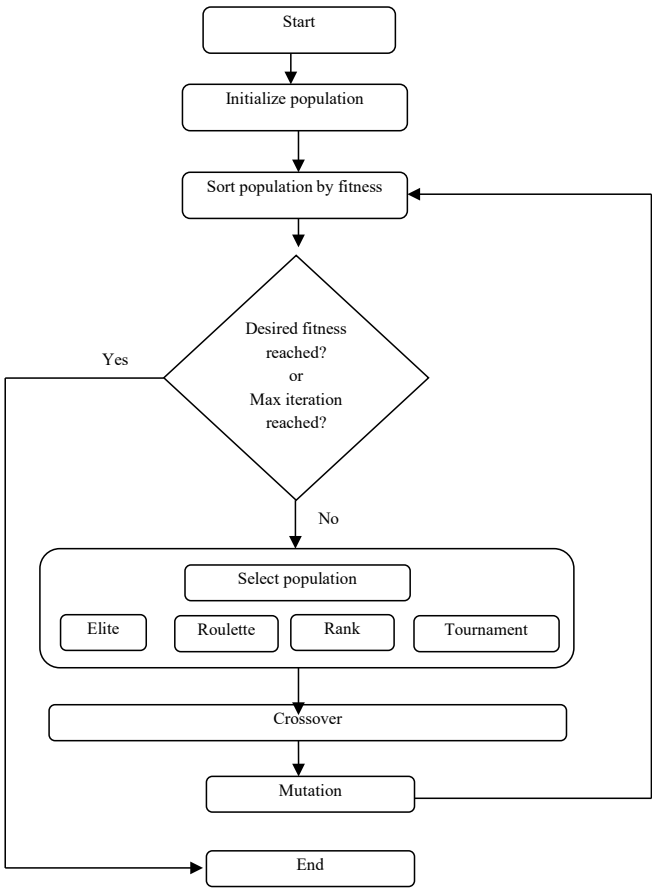


Figure 2: GA parameter optimization in SBL algorithm

population of the current generation are directly passed on to the next generation [Wan, J., Zhang, 2014]. The roulette wheel selection assigns the selection probabilities based on the classification fitness of each parameter set. The parameters are then probabilistically chosen according to their respective fitness contribution without repeating selections [Wan, J., 2012]. Another concept is rank-based selection, which sorts the parameter sets in increasing order of their classification performance [Wan, J.,, 2014] rather than assigning probabilities directly based on fitness values. In tournament selection, we randomly select a subset of size (n) from the population of candidate parameter sets and select the parameter set with the highest fitness value as a parent solution [Wan, J., 2014]. This is the optimization procedure continues iteratively until all candidate parameter combinations of the SBL framework are evaluated.

The crossover operation is used to generate new offspring solutions from the genetic information of the parent set of parameters. This process is the exchange of a part of a parent solution with a part of the other parent solution. This produces new combinations of parameters which may have better classification accuracy [Wang, G.,2010].

Algorithm 1: *SOBLA* optimization procedure

Input MRI feature samples Y, sensing matrix Φ, and partitioned training samples

Output : Optimized sparse Bayesian classification model

Initialize Ai, Bi, Γ and λ=0.001.

Repeat while (iter < max iter)

Calculate the posterior mean μ_x using equation (26)

Estimate the Toeplitz covariance matrix B using equation (30)

Normalize the covariance matrix $\hat{B}$ using equation (29)

Update the noise variance parameter λ using equation (24)

Compute the covariance matrix Σ_x using equation (25)

Optimize Equations (22)-(26) using Genetic Algorithm (GA) operations

Update the optimized sparse Bayesian para meters in the SOBLA classifier

End while

Mutation further enhances the exploration capability of the Genetic Algorithm by introducing random modifications into the parameter search space. This operation assists the optimization process in escaping local minima and increases population diversity during evolution. In the proposed framework, mutation is implemented by randomly selecting a small subset of SBL parameters and modifying specific gene values within neighbouring solution regions.

The population is split into smaller subgroups and the Genetic Algorithm is run independently on multiple processing threads to improve computational efficiency. This parallel optimization approach reduces sampling bias that may be introduced by single-threaded execution and therefore reduces computational time while improving solution quality [Wan, J.,2012]. Moreover, the periodic exchange of some SBL parameter sets between the subpopulations contributes to the diversity maintenance and the premature convergence avoidance during the optimization process.

Experimental Results

The proposed SOBLA framework was evaluated with MRI and cognitive assessment data from the Alzheimer's disease Neuroimaging Initiative (ADNI) database (www.adni.loni.usc.edu). The ADNI project aims at evaluating the combined use of longitudinal MRI, Positron Emission Tomography (PET), biological markers and neuropsychological assessment to measure the evolution of Mild Cognitive Impairment (MCI) and early AD. See www.adni-info.org for details on the ADNI initiative.

All subjects were scanned at baseline on 1.5 Tesla GE, Philips and Siemens MRI scanners. The ADNI consortium MRI Core [Wang, Y., 2010] standardized and validated the imaging protocol, using the Magnetization Prepared Rapid Acquisition Gradient Echo (MP-RAGE) protocol. Details of the MRI acquisition protocol are provided in [Weiner, M.W., 2013] and in the ADNI database documentation.

The structural MRIs that were acquired were processed with Free Surfer V4 software to obtain neuroanatomical measures of cortical and subcortical brain regions. For each cerebral hemisphere we extracted 34 cortical thickness measures from Regions of Interest (ROIs) and 15 volumetric measures from cortical and subcortical ROIs, for a total of 98 imaging features [Wipf, D.P. and Rao, 2004].

To validate the effectiveness of the proposed SOBLA classifier, performance comparisons were performed against three state-of-the-art algorithms different machine learning methods. The methods evaluated are the Correlation and Non-Linearity-aware sparse Bayesian learning model (CORNLIN) [Pishvaee, 2009], the T-MSBL-FP algorithm [Klöppel, S., 2009], and the Elastic Net algorithm [Xu, Z., 2009]. Among these approaches, T-MSBL-FP is an efficient version of the T-MSBL sparse Bayesian learning framework that leverages inter-vector correlations among regression coefficients to improve the prediction performance.

All the compared algorithms were automatically tuned in a nested cross-validation strategy during the experimental evaluation. Two types of cognitive assessment scores were used in the analysis: Alzheimer's Disease Assessment Scale (ADAS) and ADAS-P1 weighted scores. ADAS is a global cognitive assessment measure that measures the major symptoms associated with the progression of Alzheimer's disease.

Figure 3 illustrates the intermediate processing stages of the proposed framework. Figure 3(a) shows the original T1-weighted MRI input image for the ADAS sample dataset. The outputs obtained after Adaptive Median Filtering (AMF), Mean Contrast Limited Adaptive Histogram Equalization (MCLAHE) and Wavelet Transform based feature extraction are shown in Figures 3(b)–3(d) respectively.

In the first phase of the experimental analysis, the proposed SOBLA classifier which is a nonlinear prediction model is compared with three existing techniques. The cross validation prediction performance of the competing methods is presented in Table 1 . The comparative results are shown in Figure 4(a) and Figure 4(b) . The evaluation was done only based on the linear model results of the competing techniques for comparison purpose.

The results of performance evaluation obtained using three different categories of MRI measures (i.e. Left-Right Average (LR-Average), Left-Right Separate (LR-Separate) and

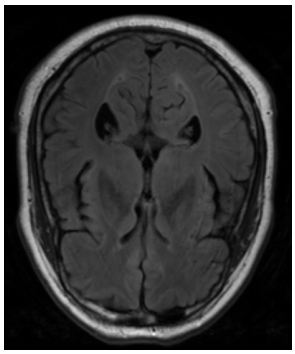


Figure 3(a): T1 examples of of an AD MRI scan

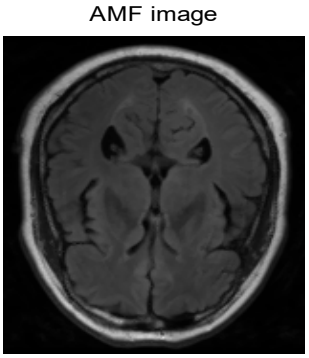


Figure 3(b): AD- T1 the study with AMF noise reduction

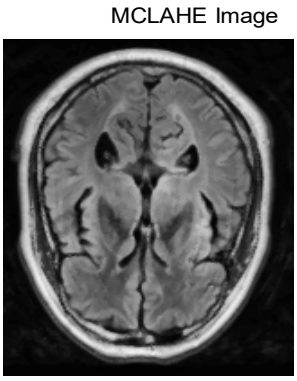


Figure 3(c): Result of improving pictures of AD- T1 sample

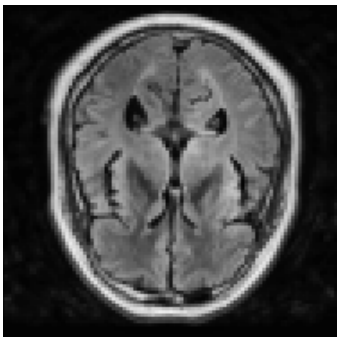


Figure 3(d): The wavelet extracting features from AD-T1 specimen outcomes

Table 1: Estimating Efficiency by Average Relativity Coefficients

Algorithms	*Types*	*ADAS*	*ADAS-P1*
Elastic Net	Linear	0.876	0.7415
	Non linear	0.761	0.7442
T-MSBL-FP	Linear	0.752	0.735
	Non linear	0.763	0.738
CORNLIN	Non linear	0.765	0.756
SOBLA	Non linear	0.778	0.762

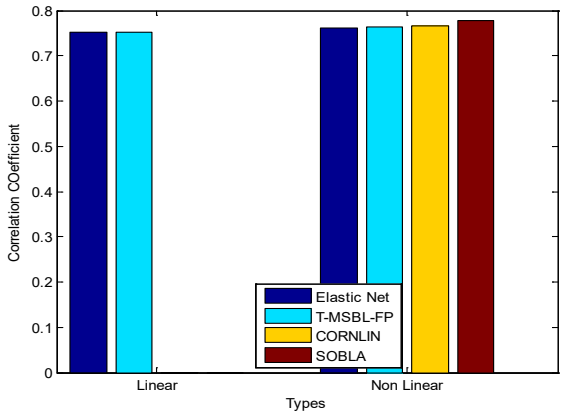


Figure 4(a): The relationship Coefficients Average vs. standard techniques (ADAS)

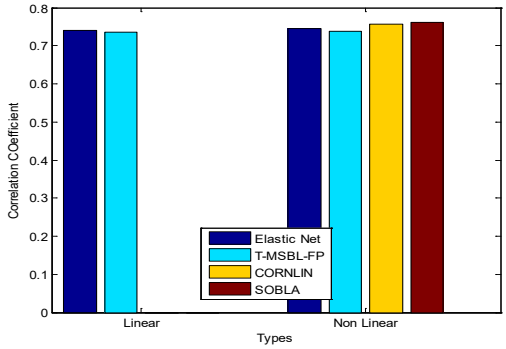


Figure 4(b): Mean of The relationship values versus methods (ADAS-P1)

Left-Right Block (LR-Block) [P. J. Bickel, 2008]) for predicting cognitive scores using existing and proposed techniques are shown here.

Table 2 shows the evaluation results in terms of mean correlation coefficient and standard error of mean (SEM) between the actual cognitive scores and the predicted scores. The experimental analysis shows that the LR-Average measures perform better prediction results than LR-Separate and LR-Block measures on both ADAS and ADAS-P1 cognitive assessment datasets.

The comparison of performance of four different classifiers is shown in figure 5 using mean correlation coefficients obtained for ADAS dataset. The three types

Table 2: Estimate outcomes (Mean ±SEM of correlation coefficients) with three MRI Measures (classifiers)

Algorithms	*Types*	*LR-Average (LR-Av)*		*LR-Separate(LR-Se)*		*LR-Block(LR-Bl)*	
		ADAS	*ADAS-P1*	*ADAS*	*ADAS-P1*	*ADAS*	*ADAS-P1*
Elastic Net	Linear	0.752 ± 0.028	0.7415 ± 0.018	0.750 ± 0.026	0.735 ± 0.0172	0.754 ± 0.022	0.708 ± 0.019
	Non linear	0.761 ± 0.0272	0.7442 ± 0.0172	0.756 ± 0.025	0.733 ± 0.0161	0.758 ± 0.0215	0.711 ± 0.0131
T-MSBL-FP	Linear	0.752 ± 0.0276	0.735 ± 0.0175	0.748 ± 0.0254	0.739 ± 0.0142	0.759 ± 0.020	0.716 ± 0.012
	Non linear	0.763 ± 0.0265	0.738 ± 0.0165	0.757 ± 0.0243	0.740 ± 0.0135	0.760 ± 0.019	0.728 ± 0.010
CORNLIN	Non linear	0.765 ± 0.024	0.756 ± 0.009	0.767 ± 0.022	0.754 ± 0.008	0.762 ± 0.018	0.765 ± 0.006
SOBLA	Non linear	0.778 ± 0.022	0.762 ± 0.008	0.780 ± 0.020	0.758 ± 0.0072	0.774 ± 0.016	0.769 ± 0.0068

of MRI measures used for evaluating the classifiers were LR-Average (LR-Av), LR-Separate (LR-Se), and LR-Block (LR-Bl). The proposed SOBLA classifier coupled with LR-Bl measure based on the results achieved outperformed the other approaches considered in terms of prediction performance and SME value.

Fig. 6. Performance comparison of four different classifiers on the ADAS-P1 dataset in terms of mean correlation coefficient values. The evaluation was carried out for the three types of the MRI measures, i.e., LR-Average (LR-Av), LR-Separate (LR-Se) and LR-Block (LR-Bl). The experimental results indicate that the proposed SOBLA classifier with LR-Bl measure achieved better prediction performance with lower Standard Mean Error (SME) compared to the other evaluated classifiers. Furthermore, the proposed SOBLA framework outperformed the prediction models based on MMSE and ADAS when compared to the LR-Bl configuration of the proposed framework for MMSE samples.

Table 3 presents the classification performance analysis by using two types of cognitive scores, i.e., Alzheimer's Disease Assessment Scale (ADAS) and ADAS-P1 weighted scores. ADAS is a general metric for cognitive evaluation that captures the primary symptoms related to the progression of Alzheimer disease. In the classification setting, the positive class is taken as the disease class and the negative class as the non-disease class. The following standard performance measures are defined for this classification structure: True Positives (TP) are positive samples that are identified correctly, True Negatives (TN) are negative samples that are identified correctly, False Positives (FP) are negative samples that are identified as positive and False Negatives (FN) are positive samples that are identified as negative. Using these classification results, standard evaluation metrics are calculated as follows:

$$\text{Sensitivity= Recall } = \frac{TP}{TP + FN} \tag{31}$$

$$\text{Specificity} = \frac{TN}{TN + FP} \tag{32}$$

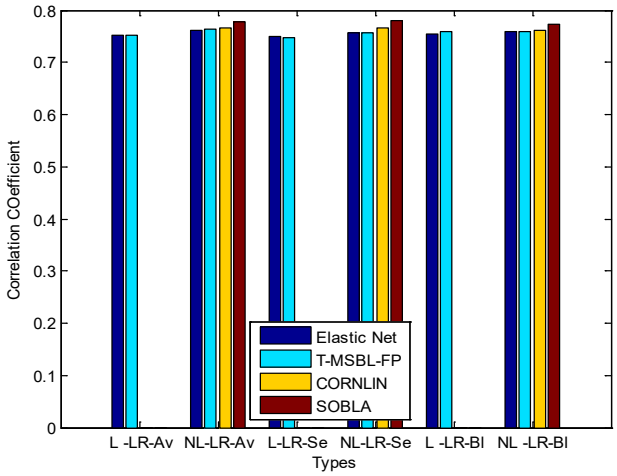


Figure 5: Indicate of standard correlated coefficients with 3 MRI Measures (classifiers- ADAS)

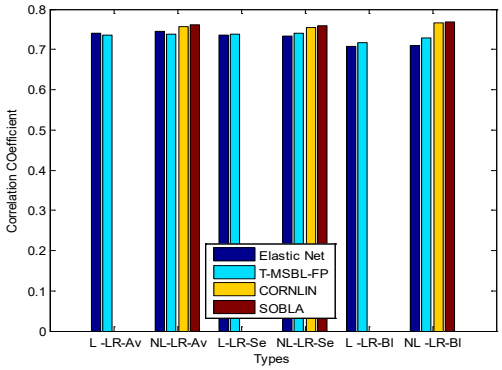


Figure 6: Mean correlation coefficients with 3 MRI Measures (classifiers-ADAS-Cog)

$$\text{Precision} = \frac{TP}{TP + FP} \tag{33}$$

$$\text{F-Measure} = 2.\ P.R/\ (P+R) \tag{34}$$

$$\text{Accuracy} = \frac{TP + TN}{TP + TN + FN + FP} \tag{35}$$

$$\text{Error rate} = 100 - \text{Accuracy} \tag{36}$$

Table 3: Recognition Efficiency with four different classifiers

Metrics	*Elastic Net*	*T-MSBL-FP*	*CORNLIN*	*SOBLA*
Sensitivity	88.25	90.21	93.4783	100
Specificity	36	30	20	0
Precision	86.12	89.25	91.4894	90
Recall	87.45	90.85	93.4783	100
F_measure	86.785	90.05	92.4731	94.7368
Accuracy	80.12	82.32	86.27	90
Error rate	19.88	17.68	13.73	10

The comparative performance analysis of the four classifiers with evaluation metrics like sensitivity, specificity, precision, recall, F-measure, and accuracy is presented in Table 3. The results obtained show that the proposed SOBLA classifier has the best detection accuracy, which is 90%. The SOBLA framework exhibited approximately 3.63%, 7.68% and 9.88% performance improvement over the CORNLIN, T-MSBL-FP and Elastic Net classifiers respectively. The proposed SOBLA approach is effective in the accurate prediction and classification of the Alzheimer's disease.

Conclusion and Future Work

- The proposed research introduced a Sparse Optimized Bayesian Learning Algorithm (SOBLA) framework for accurate prediction and classification of Alzheimer's disease using MRI-based neuroimaging data.
- The proposed method utilized intra-block correlation and inter-vector correlation in the sparse regression coefficient matrix to improve representation capability and prediction efficiency within the Bayesian learning framework.
- Image preprocessing techniques such as MCLAHE based enhancement and Adaptive Median Filtering were employed to improve MRI image quality by reducing acquisition noise, motion artifacts and intensity inhomogeneity.
- A nonlinear sparse regression mechanism combined with Genetic Algorithm (GA) optimization was integrated into the Sparse Bayesian Learning framework to improve parameter tuning, convergence and classification reliability.
- Experimental analysis conducted using the ADNI database demonstrated that the proposed SOBLA framework achieved better prediction accuracy, lower Standard Mean Error (SME) and improved classification performance compared with existing machine learning methods.
- the proposed framework successfully identified important neuroimaging biomarkers associated with cognitive impairment, and the obtained findings were consistent with previously reported clinical observations.
- Future work may focus on advanced nonlinear and deep hybrid learning models along with integration of multimodal biomedical information such as PET imaging, genomic biomarkers and longitudinal clinical data to further enhance prediction accuracy and diagnostic interpretability in Alzheimer's disease analysis.

Acknowledgements

The authors would like to thank the Department of Computer Science and Engineering, Bharathidasan University, Trichy, Tamil Nadu, for providing support and encouragement to carry out this research work.

References

A. Dale, B. Fischl, and M. Sereno, "Cortical surface-based analysis. I. Segmentation and surface reconstruction," Neuroimage, vol. 9, no. 2, pp. 179–194, 1999.

A. K. Jain, Fundamentals of Digital Image Processing. Pearson Education, 2006.

Barnes DE, Yaffe K. The projected effect of risk factor reduction on Alzheimer's disease prevalence. Lancet Neurol. 10, pp. 819–828, 2011.

Barnes, L.L., Schneider, J.A., Boyle, P.A., Bienias, J.L. and Bennett, D.A., 2006. Memory complaints are related to Alzheimer disease pathology in older persons. Neurology, 67(9), pp.1581-1585.

Bondi, M.W., Jak, A.J., Delano-Wood, L., Jacobson, M.W., Delis, D.C. and Salmon, D.P., 2008. Neuropsychological contributions to the early identification of Alzheimer's disease. Neuropsychology review, 18(1), pp.73-90.

Cha, Sung-Hyuk; Tappert, Charles C. (2009). "A Genetic Algorithm for Constructing Compact Binary Decision Trees". Journal of Pattern Recognition Research. 4 (1): 1–13.

D. Wipf, B. Rao, and S. Nagarajan, "Latent variable Bayesian models for promoting sparsity," IEEE Trans. Inf. Theory, vol. 57, no. 9, pp.6236–6255, 2011.

D. Zhang and D. Shen, "Multi-modal multi-task learning for joint prediction of multiple regression and classification variables in Alzheimer's disease," Neuroimage, vol. 59, no. 2, pp. 895–907, 2012.

D. Zhang and D. Shen, "Predicting future clinical changes of MCI patients using longitudinal and multimodal biomarkers," PLoS One, vol. 7, no. 3, pp. E33182, 2012.

Ekstrom, Michael P. Digital image processing techniques. Vol. 2. Academic Press, 2012.

H. Zou and T. Hastie, "Regularization and variable selection via the elastic net," J. R. Stat. Soc., Ser. B Stat. Methodol., vol. 67, pp.301–320, 200

Holtzman DM, Morris JC, Goate AM. Alzheimer's disease: the challenge of the second century. Sci Transl Med. 2011;3: 77sr1 .

Jack, C.R., Bernstein, M.A., Fox, N.C., Thompson, P., Alexander, G., Harvey, D., Borowski, B., Britson, P.J., L Whitwell, J., Ward, C. and Dale, A.M., 2008. The Alzheimer's disease neuroimaging initiative (ADNI): MRI methods. Journal of magnetic resonance imaging, 27(4), pp.685-691.

Khachaturian, Z.S., Petersen, R.C., Gauthier, S., Buckholtz, N., Corey-Bloom, J.P., Evans, B., Fillit, H., Foster, N., Greenberg, B., Grundman, M. and Sano, M., 2008. A roadmap for the

prevention of dementia: the inaugural Leon Thal Symposium. Alzheimer's & dementia: the journal of the Alzheimer's Association, 4(3), pp.156-163.

Klöppel, S., Stonnington, C.M., Barnes, J., Chen, F., Chu, C., Good, C.D., Mader, I., Mitchell, L.A., Patel, A.C., Roberts, C.C. and Fox, N.C., 2008. Accuracy of dementia diagnosis—a direct comparison between radiologists and a computerized method. Brain, 131(11), pp.2969-2974.

Klöppel, S., Stonnington, C.M., Chu, C., Draganski, B., Scahill, R.I., Rohrer, J.D., Fox, N.C., Jack Jr, C.R., Ashburner, J. and Frackowiak, R.S., 2008. Automatic classification of MR scans in Alzheimer's disease. Brain, 131(3), pp.681-689.

Korolev IO. Alzheimer's Disease: A Clinical and Basic Science Review. Medical Student Research Journal. 2014;4: 24–33.

L. Lin, N. J. Higham, and J. Pan, "Covariance structure regularization via entropy loss function," Computat. Statist. Data Anal., vol. 72, pp. 315–327, 2014.

N. M. Razali and J. Geraghty, "Genetic algorithm performance with different selection strategies in solving TSP," Proceedings of the World Congress on Engineering (WCE '11), vol. 2, pp. 1134–1139, London, UK, 2011.

P. J. Bickel and E. Levina, "Regularized estimation of large covariance matrices," Ann. Stat., pp. 199–227, 2008.

Petersen, R.C., Roberts, R.O., Knopman, D.S., Boeve, B.F., Geda, Y.E., Ivnik, R.J., Smith, G.E. and Jack, C.R., 2009. Mild cognitive impairment: ten years later. Archives of neurology, 66(12), pp.1447-1455.

Pishvaee, M.S., Jolai, F. and Razmi, J., 2009. A stochastic optimization model for integrated forward/reverse logistics network design. Journal of Manufacturing Systems, 28(4), pp.107-114.

R. C. Gonzalez, R. E. Woods and S. L. Eddins, Digital Image Processing Using MATLAB. Pearson Education, 2005.

Reisberg, B., Shulman, M.B., Torossian, C., Leng, L. and Zhu, W., 2010. Outcome over seven years of healthy adults with and without subjective cognitive impairment. Alzheimer's & dementia: the journal of the Alzheimer's Association, 6(1), pp.11-24.

Risacher, S.L., Saykin, A.J., Wes, J.D., Shen, L., Firpi, H.A. and McDonald, B.C., 2009. Baseline MRI predictors of conversion from MCI to probable AD in the ADNI cohort. Current Alzheimer Research, 6(4), pp.347-361.

S. Zhang, X. Xue, X. Zhang, Feature extraction and classification with wavelet transform and support vector machines, in: Proceedings IEEE International Geoscience and Remote Sensing Symposium, IGARSS '05, vol. 6, 2005, pp. 3795–3798.

Sabuncu, M.R. and Van Leemput, K., 2012. The relevance voxel machine (RVoxM): a self-tuning Bayesian model for informative image-based prediction. IEEE transactions on medical imaging, 31(12), pp.2290-2306.

Sasi, N.M. and Jayasree, V.K., 2013. Contrast limited adaptive histogram equalization for qualitative enhancement of myocardial perfusion images. Engineering, 5(10), pp. 326-331.

Shen, L., Qi, Y., Kim, S., Nho, K., Wan, J., Risacher, S.L. and Saykin, A.J., 2010, Sparse bayesian learning for identifying imaging biomarkers in AD prediction. In International Conference on Medical Image Computing and Computer-Assisted Intervention, pp. 611-618.

Slavin, M.J., Brodaty, H., Kochan, N.A., Crawford, J.D., Trollor, J.N., Draper, B. and Sachdev, P.S., 2010. Prevalence and predictors of "subjective cognitive complaints" in the Sydney Memory and Ageing Study. The American Journal of Geriatric Psychiatry, 18(8), pp.701-710.

Stonnington, C.M., Chu, C., Klöppel, S., Jack Jr, C.R., Ashburner, J., Frackowiak, R.S. and Alzheimer Disease Neuroimaging Initiative, 2010. Predicting clinical scores from magnetic resonance scans in Alzheimer's disease. Neuroimage, 51(4), pp.1405-1413.

Vounou, M., Janousova, E., Wolz, R., Stein, J.L., Thompson, P.M., Rueckert, D., Montana, G. and Alzheimer's Disease Neuroimaging Initiative, 2012. Sparse reduced-rank regression detects genetic associations with voxel-wise longitudinal phenotypes in Alzheimer's disease. Neuroimage, 60(1), pp.700-716.

Wan, J., Zhang, Z., Rao, B.D., Fang, S., Yan, J., Saykin, A.J. and Shen, L., 2014. Identifying the neuroanatomical basis of cognitive impairment in Alzheimer's disease by correlation- and nonlinearity-aware sparse Bayesian learning. IEEE transactions on medical imaging, 33(7), pp.1475-1487.

Wan, J., Zhang, Z., Yan, J., Li, T., Rao, B.D., Fang, S., Kim, S., Risacher, S.L., Saykin, A.J. and Shen, L., 2012, Sparse Bayesian multi-task learning for predicting cognitive outcomes from neuroimaging measures in Alzheimer's disease. In Computer Vision and Pattern Recognition (CVPR), pp. 940-947.

Wang, G., Li, D., Pan, W. and Zang, Z., 2010. Modified switching median filter for impulse noise removal. Signal Processing, 90(12), pp.3213-3218.

Wang, Y., Fan, Y., Bhatt, P. and Davatzikos, C., 2010. High-dimensional pattern regression using machine learning: from medical images to continuous clinical variables. Neuroimage, 50(4), pp.1519-1535.

Weiner, M.W., Veitch, D.P., Aisen, P.S., Beckett, L.A., Cairns, N.J., Green, R.C., Harvey, D., Jack, C.R., Jagust, W., Liu, E. and Morris, J.C., 2013. The Alzheimer's Disease Neuroimaging Initiative: a review of papers published since its inception. Alzheimer's & dementia: the journal of the Alzheimer's Association, 9(5), pp.e111-e194.

Wipf, D.P. and Rao, B.D., 2004. Sparse Bayesian learning for basis selection. IEEE Transactions on Signal processing, 52(8), pp.2153-2164.

Xu, Z., Liu, X. and Ji, N., 2009, Fog removal from color images using contrast limited adaptive histogram equalization. In 2nd International Congress on Image and Signal Processing, 2009(CISP'09), pp. 1-5.